

Conf-690429-1

Second L. H. Gray Conference

8-11 April 1969

Particle Tracks in Condensed Matter*

Robert Katz and E. J. Klobetich[†]

Behlen Laboratory of Physics

University of Nebraska

Lincoln, Nebraska 68508

MASTER

Abstract:

A proposed theory of track formation attributes observed effects to the spatial deposition of energy by secondary electrons. The theory is compared to experimental observations in a variety of fields, with good results. In contrast, linear measures of the interaction of charged particles with matter (LET, primary excitation, primary ionization, restricted energy loss) are unsuitable parameters through which to describe particle tracks, except in limiting cases, because many detection media are saturable. Energy deposited close to a particle's path often produces a disproportionately small response, because of "overkill".

*Supported by the U. S. Atomic Energy Commission and the National Science Foundation

[†]Present Address: H. H. Wills Physics Laboratory, University of Bristol

LEGAL NOTICE

This report was prepared as an account of Government sponsored work. Neither the United States, nor the Commission, nor any person acting on behalf of the Commission:

A. Makes any warranty or representation, expressed or implied, with respect to the accuracy, completeness, or usefulness of the information contained in this report, or that the use of any information, apparatus, method, or process disclosed in this report may not infringe privately owned rights; or

B. Assumes any liabilities with respect to the use of, or for damages resulting from the use of any information, apparatus, method, or process disclosed in this report.

As used in the above, "person acting on behalf of the Commission" includes any employee or contractor of the Commission, or employee of such contractor, to the extent that such employee or contractor of the Commission, or employee of such contractor prepares, disseminates, or provides access to, any information pursuant to his employment or contract with the Commission, or his employment with such contractor.

DISTRIBUTION OF THIS DOCUMENT IS UNLIMITED

JEP

DISCLAIMER

This report was prepared as an account of work sponsored by an agency of the United States Government. Neither the United States Government nor any agency Thereof, nor any of their employees, makes any warranty, express or implied, or assumes any legal liability or responsibility for the accuracy, completeness, or usefulness of any information, apparatus, product, or process disclosed, or represents that its use would not infringe privately owned rights. Reference herein to any specific commercial product, process, or service by trade name, trademark, manufacturer, or otherwise does not necessarily constitute or imply its endorsement, recommendation, or favoring by the United States Government or any agency thereof. The views and opinions of authors expressed herein do not necessarily state or reflect those of the United States Government or any agency thereof.

DISCLAIMER

Portions of this document may be illegible in electronic image products. Images are produced from the best available original document.

I. Introduction

To a large extent, the damage to condensed matter from gamma-ray irradiation and charged particle bombardment is due to the interaction of secondary electrons with the medium, so that differences in the observed effects arise from the time scale with which the secondary electrons are generated and from their spatial distribution. The energy deposition from secondary electrons gives rise to excitations, to bond rupture, to molecular and crystallographic rearrangements which are detected in different ways, of which the alteration of biological function may be the most specific. In small subvolumes near an ion's path we assume that the response of the medium to a passing ion is as if the subvolume were part of a larger system uniformly irradiated with gamma-rays to the same average energy deposition. Thus, knowledge of the response function of a medium to gamma rays may be coupled with knowledge of the spatial distribution of the energy deposited by secondary electrons about an ion's path, to yield the spatial distribution of response, and therefore the total response of the medium to a single charged particle.

Several detection systems have been analyzed on this basis.

An assumption of exponential response (one-or-more hit in the cumulative Poisson distribution) to dose has been used to describe particle tracks in emulsion, the scintillation

pulse heights in NaI(Tl), and the RBE for dry enzymes and viruses.

An assumption of threshold response (many-hit in the cumulative Poisson distribution) has been used to correlate observations of the formation of etchable tracks in dielectrics.

Since experimental data represent average responses of the medium to the passing charged particle, as when one measures the blackness of the particle's track in emulsion, or its grain count, theories of track formation must predict average response. In the present work, the average is taken at the level of the energy deposition by secondary electrons. We make no attempt to follow the paths of individual electrons as they meander through the medium. So long as the theory predicts correctly the mean probability for the production of detection events as a function of radial distance from the ion's path, the fact that these events really lie along the path of a secondary electron may be inconsequential to the successful application of the theory.

II. Spatial Distribution of Ionization Energy

To find the spatial distribution of ionization energy about the path of a charged particle, electron data have been combined with the delta-ray distribution formula, and an assumed angular distribution of the ejected secondary electrons (delta-rays).

Electron energy dissipation data for a range of materials and energies have been summarized into computer algorithms, in excellent agreement with experimental data, from 20 keV to 2 MeV (Kobetich and Katz 1968-1,1969). These algorithms have been used for extrapolation to low electron energies, as needed.

In all computations, the delta-ray distribution formula differential in energy, and calculated for the interaction of an incident charged particle with free electrons, is used. It is assumed that the energy which would be given to a free electron is the energy transferred to the bound electron.

Where interest centers on effects close to an ion's path, say within 1,000 Å, all delta rays are taken to be ejected normally, for most of the significant energy deposition is associated with low energy delta-rays, ejected in grazing collisions. Normal ejection has been used in the analysis of RBE (Butts and Katz 1967), NaI(Tl) (Katz and Kobetich 1968-1), and the formation of etchable tracks in dielectrics (Katz and Kobetich 1968-2).

Where the events of interest are microns distant from the ion's path, the angular distribution has been adjusted to give best agreement with experimental data. Track formation in emulsion has been studied through the use of a distribution of the form $5 \cos^4 \theta$ (Kobetich and Katz 1968-2), and the classical distribution for the encounter of a heavy particle with a free electron (Katz and Kobetich 1969). Fortunately

the results of the theory are insensitive to the details of the angular distribution. Indeed the principal results seem to derive from the fact that under reasonable assumptions of angular distribution or energy dissipation by delta rays, the spatial distribution of the energy is nearly inversely proportional to the square of the distance from the ion's path, and nearly inversely proportional to the square of the ion's speed, and directly proportional to the square of its effective charge (accomodating for electron capture and loss).

In all applications of the theory up to the present time, the direct excitation of the medium by the passing ion has been neglected. In essence the model was initially developed for the study of the tracks of energetic heavy ions in emulsion (Katz and Butts 1965) where this assumption is clearly valid, and has been applied to other situations where this neglect might be thought to generate difficulty. Nevertheless, in only two cases have possible difficulties appeared. The model does not predict the relativistic rise in grain counts or bubble counts from the tracks of singly charged particles, nor does it properly yield pulse height for proton or alpha particle bombardments of NaI(Tl). The neglect of direct excitations may be responsible for these failures. The validity of the neglect may be due to "overkill", for the response of a medium is saturable, and a small fraction of the response may result from the large fraction of the energy loss to be associated with direct excitation.

III. Results

The present theory of track formation asserts that track formation must be understood from the spatial distribution of ionization energy deposited by secondary electrons about the path of a charged particle. Such an assertion implies that track formation cannot be understood from linear measures of charged particle interaction, for these have no explicit knowledge of spatial effects. The LET, and similar parameters cannot properly describe track formation.

Data from several sources confirm this view. Thus the light pulse from a scintillation counter is not proportional to the specific energy loss, the specific energy loss is not a good parameter for describing the formation or non-formation of etchable tracks in dielectrics, but the most spectacular demonstration arises from particle tracks in emulsion, shown in Fig. 1, where for an energetic iron ion, the maximum silver development occurs at a range of around 1,000 microns, but the maximum of the energy loss occurs at a range of about 25 microns. The appearance of the track simply does not follow from linear energy loss considerations. In Fig. 2 we note that the change in emulsion sensitivity changes the response of the emulsion to ions in a qualitative way. The response of the medium simply does not scale with its sensitivity- the very character of the response is altered.

To describe the formation of particle tracks in emulsion we first find the point distribution of energy, as in Fig. 3, and then average this distribution over the size of a sphere approximating an emulsion grain, as shown in Fig. 4. The two distributions approach each other beyond two sphere radii from the ion's path, so that where grain sensitization at distances larger than a grain diameter is significant, Fig. 3 may be used instead of Fig. 4 to represent the mean dose received by the grain. In earlier work this has been called "the point target approximation" (Butts and Katz 1967).

When the response of the medium is exponential (1-hit) we take the probability P for the sensitization of an emulsion grain to be represented by the expression

$$P(t) = 1 - \exp(-\bar{E}(t)/E_0) \quad (1)$$

where $\bar{E}(t)$ is the mean energy density deposited in a grain whose center is at distance t from the ion's path (Fig. 4), and E_0 (also called the D-37 dose) is the characteristic dose for activation of 63% of the emulsion grains in an emulsion uniformly exposed to gamma-rays. A single parameter, E_0 , accommodates variations in emulsion and in processing. Eq. (1) has also been used to describe NaI(Tl) and RBE. Combined with Fig. 4, it yields the spatial distribution of developed grains, and can therefore be used as the basis of a calculation of the microdensitometry of particle tracks in emulsion, with results shown in Fig. 5.

The appearance of a heavy ion track in emulsion may also be characterized by its "width", measured by manually tracing around track segments, and dividing the included area in a segment by its length. We compare the measured width to $2t$, found theoretically by taking $P = 0.4$, in Fig. 6.

Rapidly moving singly charged particles do not form a closed track. Observers make grain or gap counts, which they convert into grain counts by statistical procedures. An observer must decide which grain belongs to a track and which is background, and typically decides that grains whose center is beyond some characteristic distance, τ , do not belong to the track. We therefore integrate Eq. (1) from 0 to τ to find the theoretical grain count cross section, and compare these calculations to experimental data in Figs. 7 and 8. We find (Katz and Klobetich 1969) that the number of grains per unit length g is related to the maximum observable number, g_{sat} , by the expression

$$g = g_{\text{sat}} [1 - \exp(-\alpha z^2 / \beta^2 E_0)] \quad (2)$$

where $\alpha z^2 / \beta^2$ is the mean value of \bar{E} within the cylinder of radius τ , and βc is the speed of the ion. When we plot Eq. (2) against the restricted energy loss in silver bromide, as in Fig. 9, we see that the proportionality between grain count and restricted energy loss depends on the emulsion sensitivity and the particle speed. The curve bears an intimate relationship to a conceptual structure used in radiobiology,

where it might be interpreted as a plot of "efficiency factor" against LET.

If Eq. (1) is integrated over all t , we find the cross section for the total response of the medium to charged particle bombardment, and, using parameters appropriate to the medium of interest and the detection techniques, we find the relative pulse heights produced by heavy ions in NaI(Tl), as in Fig. 10, or the inactivation cross sections for dry enzymes and viruses, as in Fig. 11. It is only in the last figure that experimental data for both the cross-section and the characteristic dose are known from experiment. In all other cases the characteristic dose must be determined by trial.

The phenomena described above are treated with a single model, with minor variations.

For the formation of etchable tracks in dielectrics, the spatial distribution of the energy deposited by delta rays again appears to be determining. A simple model which supposes that track formation or non-formation is to be associated with a criterion of minimal dosage at a minimal distance is found to be in good agreement with experiment, as shown in Fig. 12 (Katz and Kobetich 1968-2). If the critical distance is taken as $2 \times 10^{-7} \text{ g/cm}^2$, an energy deposition of about $8 \times 10^8 \text{ erg/g}$ is the minimal dosage in Lexan polycarbonate. As consistent with views expressed earlier about the relationship between gamma-ray and charged particle bombardment, the minimal dosage for track formation is a dosage producing

macroscopic damage when this material is irradiated with gamma-rays.

IV. Discussion

From the variety of phenomena described by the present theory of track structure, and the quantitative agreement between theory and experiment, we must conclude that the theory encompasses many of the essential features of track formation, though details in the calculation of the energy deposition, or in the assignment of the critical energy dose will be altered with improved knowledge. The energy deposition in average small subvolumes (microdose) around the path of an ion is taken to be the significant parameter. The theory asserts that track structure can only be understood from the spatial distribution of the microdose, and from the response function of the medium.

Finally, the present theory of track formation enables us to compare the relative sensitivities of different detecting systems in terms of the critical energy dosage for track formation, and the estimated radius of a sensitive volume, as shown in Table 1. The critical dose varies over 5 or 6 orders of magnitude for the different detectors thus far studied, but when this dose is multiplied by the volume of the sensitive site, it appears that an energy deposition ranging from 3 to 300 eV is required to sensitize these detectors.

Table 1

Sensitivity of Detecting Systems

<u>1-hit</u>	<u>E_0</u>	<u>a_0</u>
	erg cm^{-3}	cm
G-5 emulsion	1.5×10^4	1.5×10^{-5}
K-5 emulsion	5.0×10^4	1.0×10^{-5}
NaI(Tl)	4.0×10^7	3.3×10^{-7}
T-1 Phage	5.7×10^7	6×10^{-7}
Trypsin	3.6×10^9	2×10^{-7}

<u>many-hit</u>	<u>critical dose</u>
	erg g^{-1}
cellulose nitrate	3×10^8
Lexan polycarbonate	7×10^8
mica	3×10^9
olivine	1×10^{10}

References

Barkas, W. H. 1963, Nuclear Research Emulsions, Academic Press, N.Y.

Butts, J.J. and Katz, R., 1967, Radiation Research 30, 855

Fowler, P. H. 1969 , private communication

Katz, R. and Butts, J.J., Phys. Rev. 137, B198

Katz, R. and Kobetich, E.J., 1968-1, Phys. Rev. 170, 397

Katz, R. and Kobetich, E. J. 1968-2, Phys. Rev. 170, 401

Katz, R. and Kobetich, E. J. 1969, to be published

Kobetich, E. J. and Katz, R. 1968-1, Phys. Rev. 170, 391

Kobetich, E. J. and Katz, R. 1968-2, Phys. Rev. 170, 405

Kobetich, E. J. and Katz, R. 1969, Nuclear Instruments and Methods, in press

Powell, C.F., Fowler, P.H., and Perkins, D. H. 1959, The Study of Elementary Particles by the Photographic Method, Pergamon Press, N.Y.

Captions

Fig. 1 Track of an iron nucleus in G-5 emulsion, with residual range, energy, and β ($= v/c$) shown. The maximum specific energy loss occurs at a residual range of about 25 microns. (courtesy P. H. Fowler)

Fig. 2. Tracks of 400 MeV argon ions in emulsions of different sensitivities. The silver deposited does not scale with sensitivity. There are qualitative differences in response between the most sensitive and the least sensitive emulsions. The Bragg peak occurs at a range of about 15 microns. Note that only in the least sensitive emulsion does the amount of deposited silver seem to follow the Bragg curve.
(Barkas 1963)

Fig. 3 Point distribution of the energy deposition in emulsion by delta rays, divided by the square of the effective charge, as a function of t , the distance from the path of an ion moving at speed βc . For this calculation the angular distribution implied by classical kinematics was used.
(Katz and Kobetich 1969)

Fig. 4. Spatial distribution of the average energy deposited in spheres of radius 0.2 microns, divided by the square of the effective charge, as a function of the distance t of the center of the sphere from the ion's path, in emulsion.
(Katz and Kobetich 1969)

Fig. 5 Blackness variation as a function of distance from the ion's path calculated for ions of atomic number 26, 80, 90, 100, 110, and 120, moving at $\beta = 0.95$. These calculations are normalized so as to agree with measurements (Fowler 1969) of relativistic iron tracks in emulsion. Measurements of the tracks of very heavy cosmic ray particles are shown. Agreement in the slopes of the curves implies that the calculations of spatial distribution of the energy is in reasonable agreement with blackness measurement at very large distances from the path of an ion. Final Z identification of these particles depends on knowledge of E_0 and β . (Katz and Klobetich 1969).

Fig. 6 Measurements of the width of three tracks in a stack of G-5 emulsion exposed at balloon altitudes, bracketed between theoretical curves of the indicated Z, at indicated values of E_0 and P. The divergence between theory and measurement at low range is expected, for the tracks are very dense in this region, and it is not possible to locate the experimental value of t at which $P = 0.4$ (see Fig. 1). (Katz and Klobetich 1969)

Fig. 7 Measured grain count for singly charged particles in K-5 emulsion, shown against calculations from Eq. (2). (Barkas 1963, Katz and Klobetich 1969)

Fig. 8 Grain counts for relativistic ions in G-5 emulsion as a function of z^2 (Powell et al 1959) shown against ϵ curves from Eq. (2) at $\beta = 0.95$. Solid circles A and hollow circles B are from emulsions representing the limits of normal development, while hollow squares C are from underdeveloped emulsion. Note that variations in processing are accommodated by variations in E_0 alone. (Katz and Kobetich 1969). Points flagged with a cross, at $z^2 = 16$ and 25 would fit the theoretical curves if experimentally assigned Z values were off by 1. Experimentally, the value of Z and β are unknown and interact in the Z assignment.

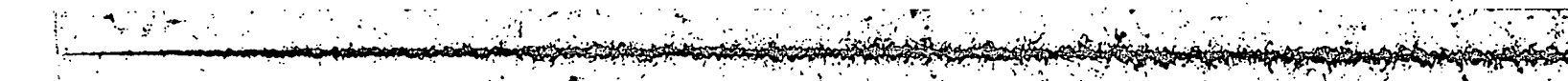
Fig. 9 Grain count is plotted against restricted energy loss in AgBr (Barkas 1963), from Eq. (2). The grain count expected from average development of G-5 emulsion is shown in curve A, from average development of K-5 emulsion in curve B, and from underdeveloped G-5 emulsion in curve C. Lines at 45° tangent to these curves are shown, where grain count is proportional to restricted energy loss. Note that even where the track is linear, linear measures of the energy loss do not describe the observed effect well.

Fig. 10 Experimental values of the relative pulse heights generated in NaI(Tl) by ions of varying incident energies (light lines) are compared to theory (heavy lines). (Katz and Kobetich 1968-1).

Fig. 11 Theoretical relationship between the cross section for heavy ion inactivation and the D-37 dose for gamma-rays, for dry enzymes and viruses. Unadjusted experimental data (references cited in Butts and Katz 1967) are plotted over theoretical curves derived from the energy dissipation algorithm of Kobetich and Katz 1968-1. Horizontal error bars on T-1 phage points show the range of D-37 data for this material.

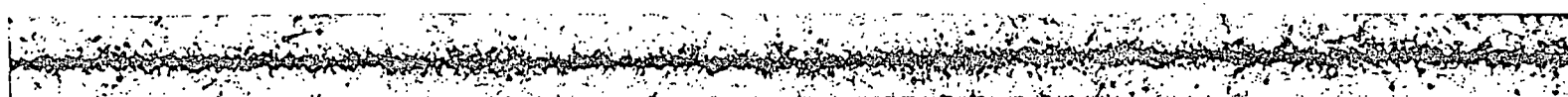
Fig. 12 Dosage of ionization energy in Lexan polycarbonate at $2 \times 10^{-7} \text{ gcm}^{-2}$, with superimposed data from two observers plotted as solid figures if etchable tracks are formed, and as hollow figures if not. The two adjacent horizontal lines are thresholds for track formation for the two sets of data. Shading along the dose axis is open if the indicated gamma-ray dose gives negligible damage, is cross hatched if it produces moderate damage, and is solid if the indicated dose produces sever damage to a variety of physical properties of the bulk material. (Katz and Kobetich 1968-2)

26 Fe 56

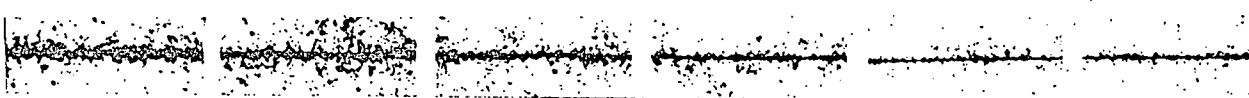


$R = 0$ 100μ 200 300 400 500μ
 $E =$ 4.4 GeV 1.7 GeV
 $\beta =$ 0.13 0.25

1000μ 1500μ
 2.8 GeV 3.7 GeV
 0.31 0.36



$R = 1500\mu$ 2000μ 2500μ 3000μ
 $E = 3.7 \text{ GeV}$ 4.5 GeV 5.2 GeV 5.8 GeV
 $\beta = 0.36$ 0.39 0.42 0.44



$R = 3000\mu$ 5mm 1cm 2cm 4cm 6cm
 $E = 5.8 \text{ GeV}$ 8 GeV 12 GeV 19 GeV 29 GeV 38 GeV
 $\beta = 0.44$ 0.49 0.58 0.68 0.76 0.82

ARGON

in

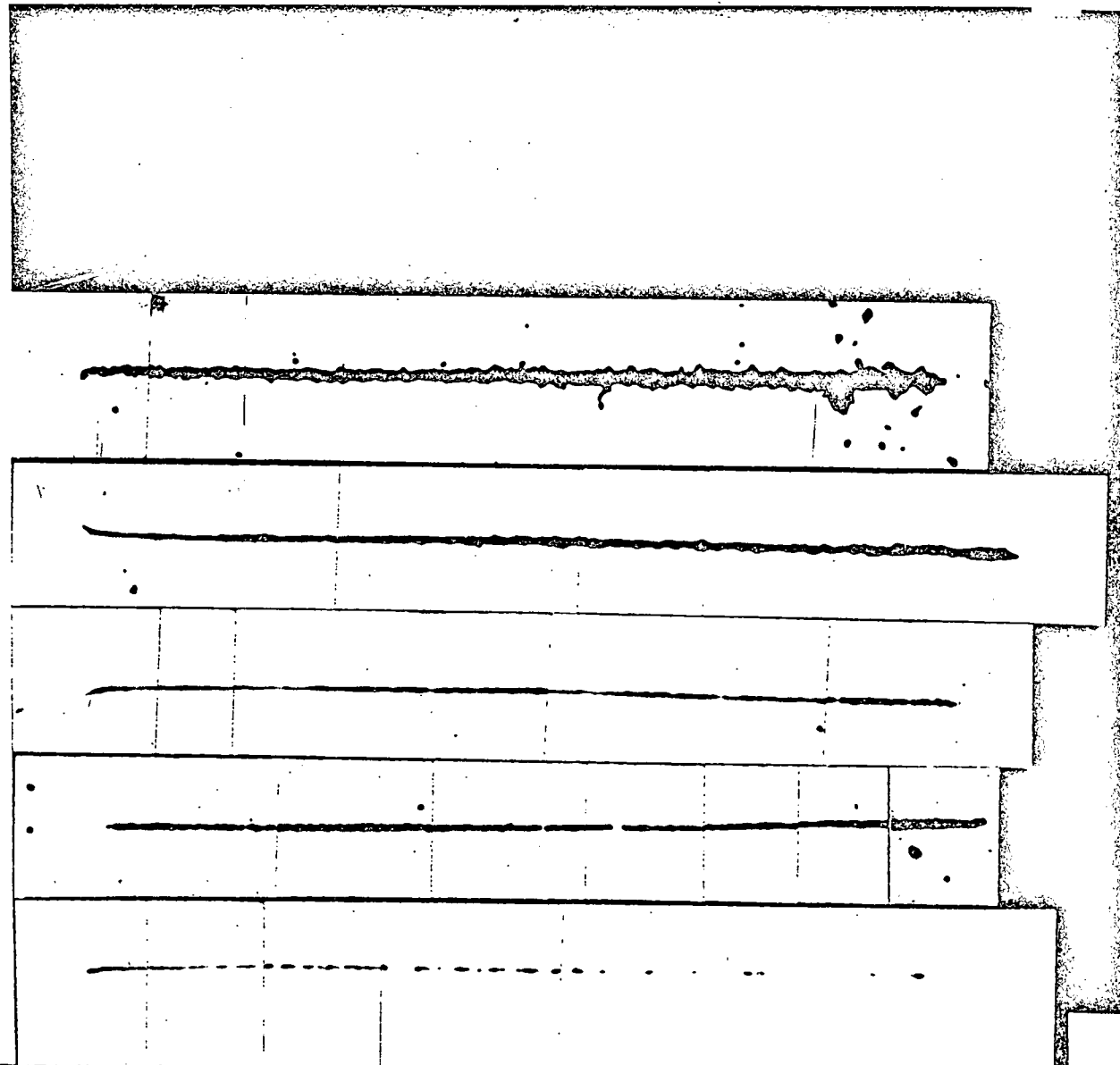
G.5

C.2

D.1

K minus 1

K minus 2



100 μ

Fig. 2 18

Fig. 3

19

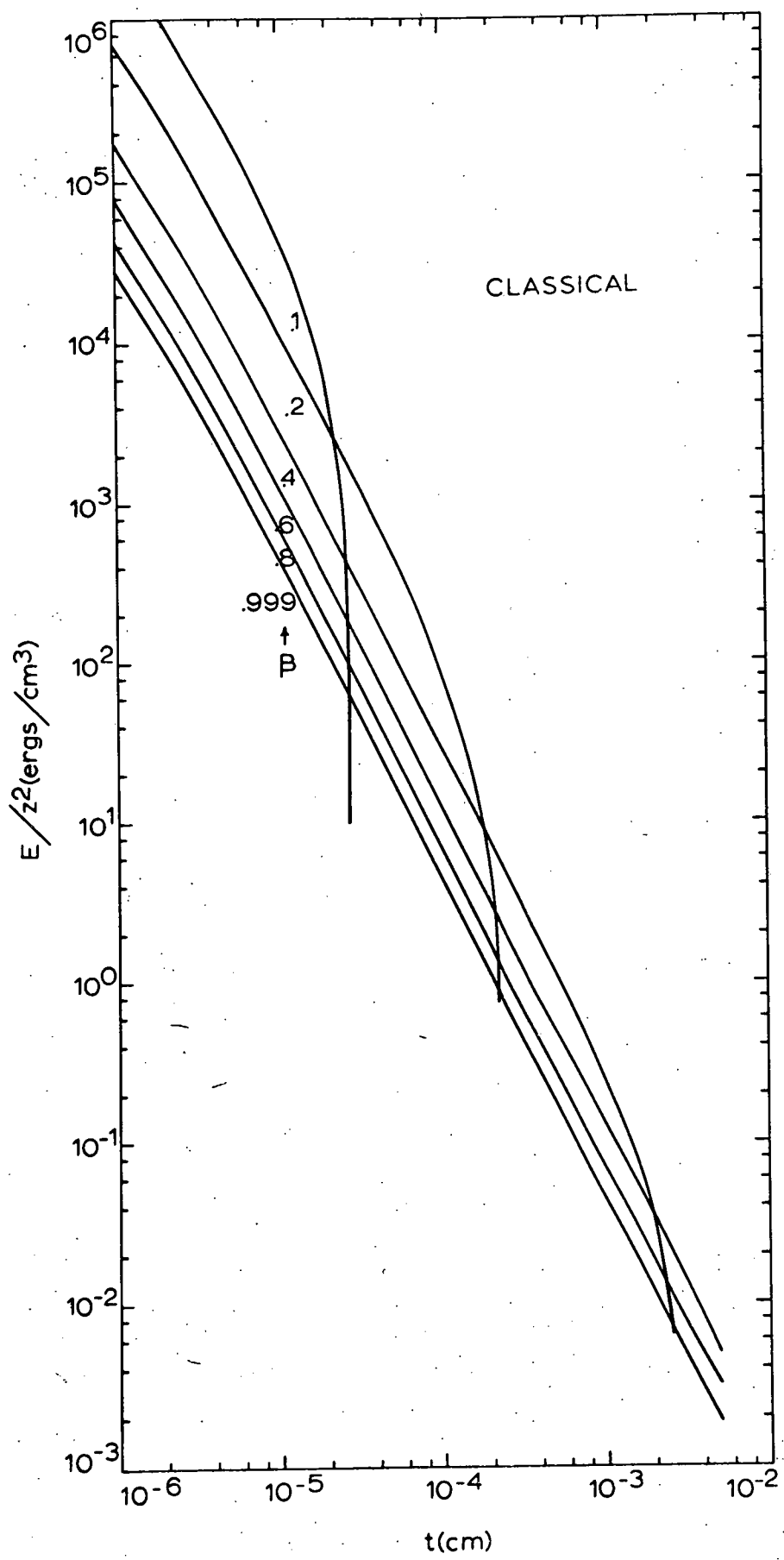
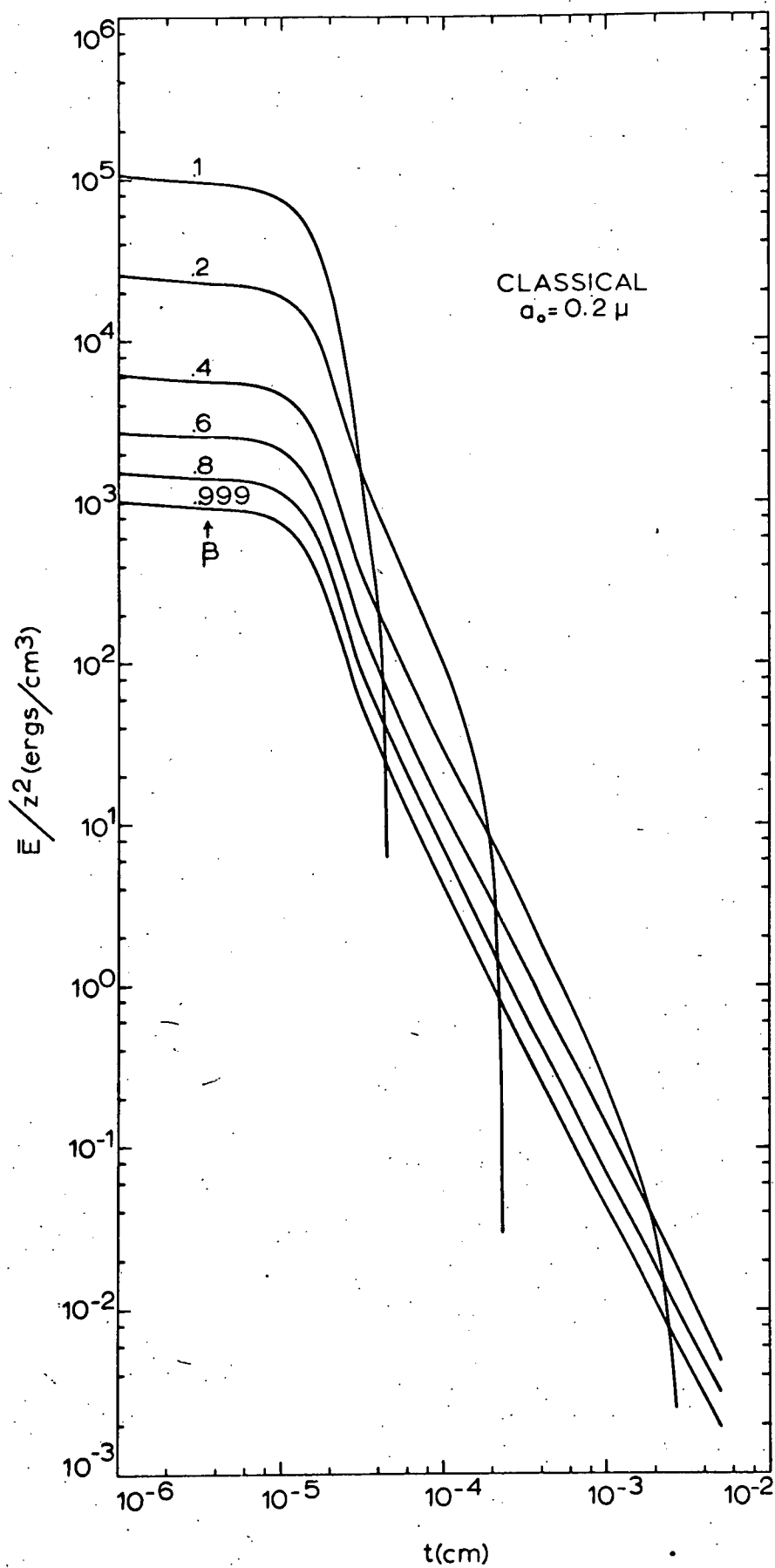
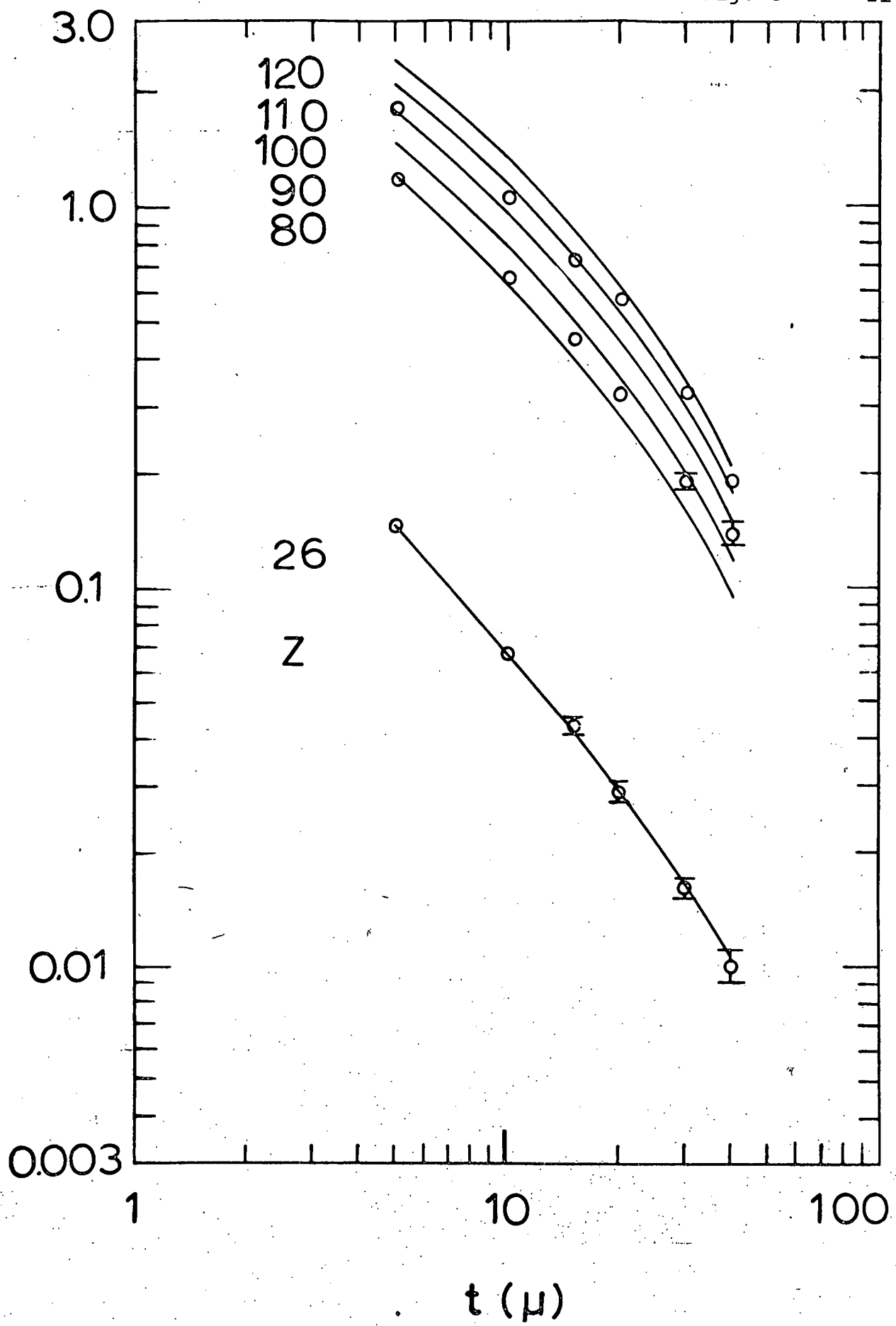


Fig. 4

20



NORMALIZED BLACKNESS



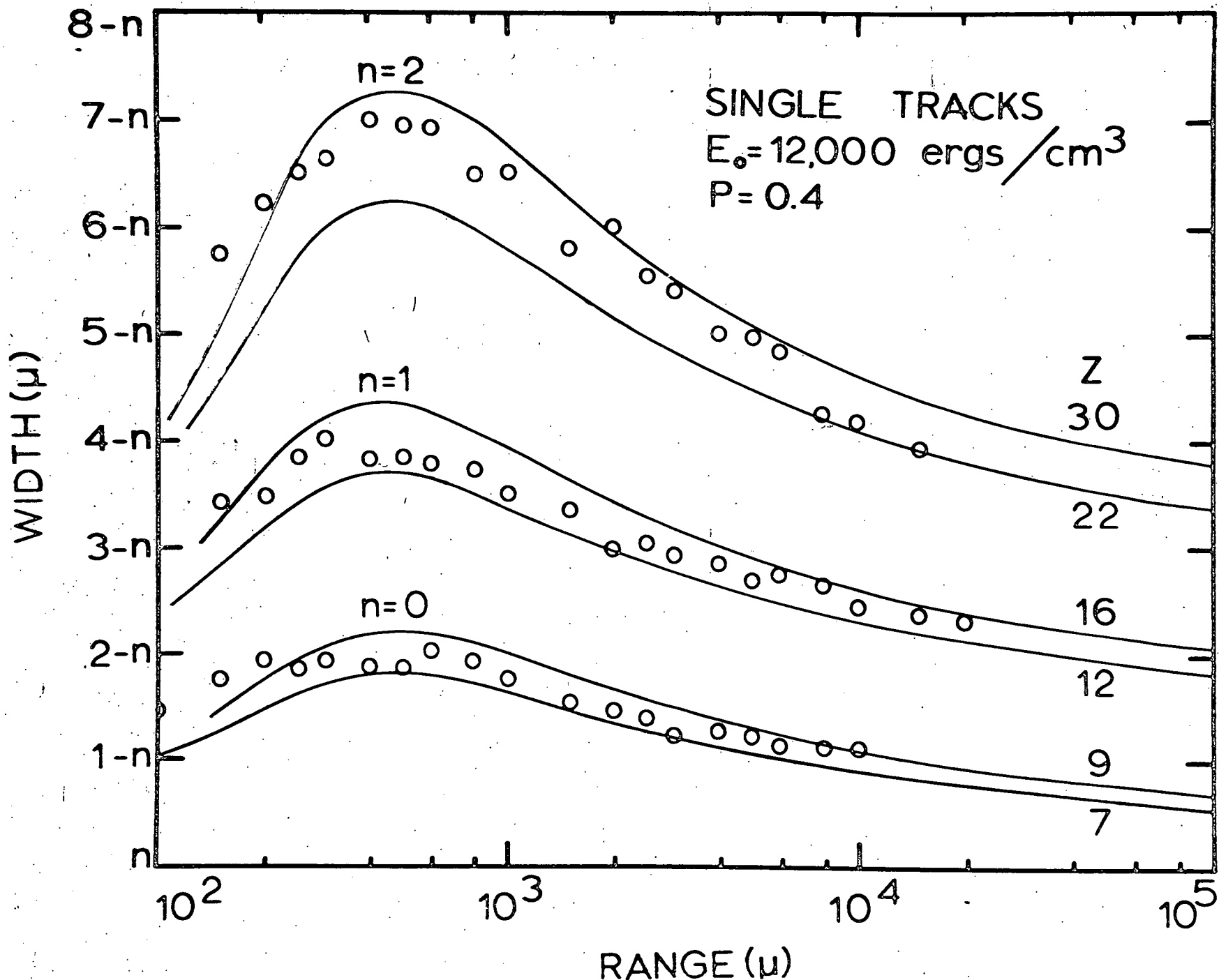
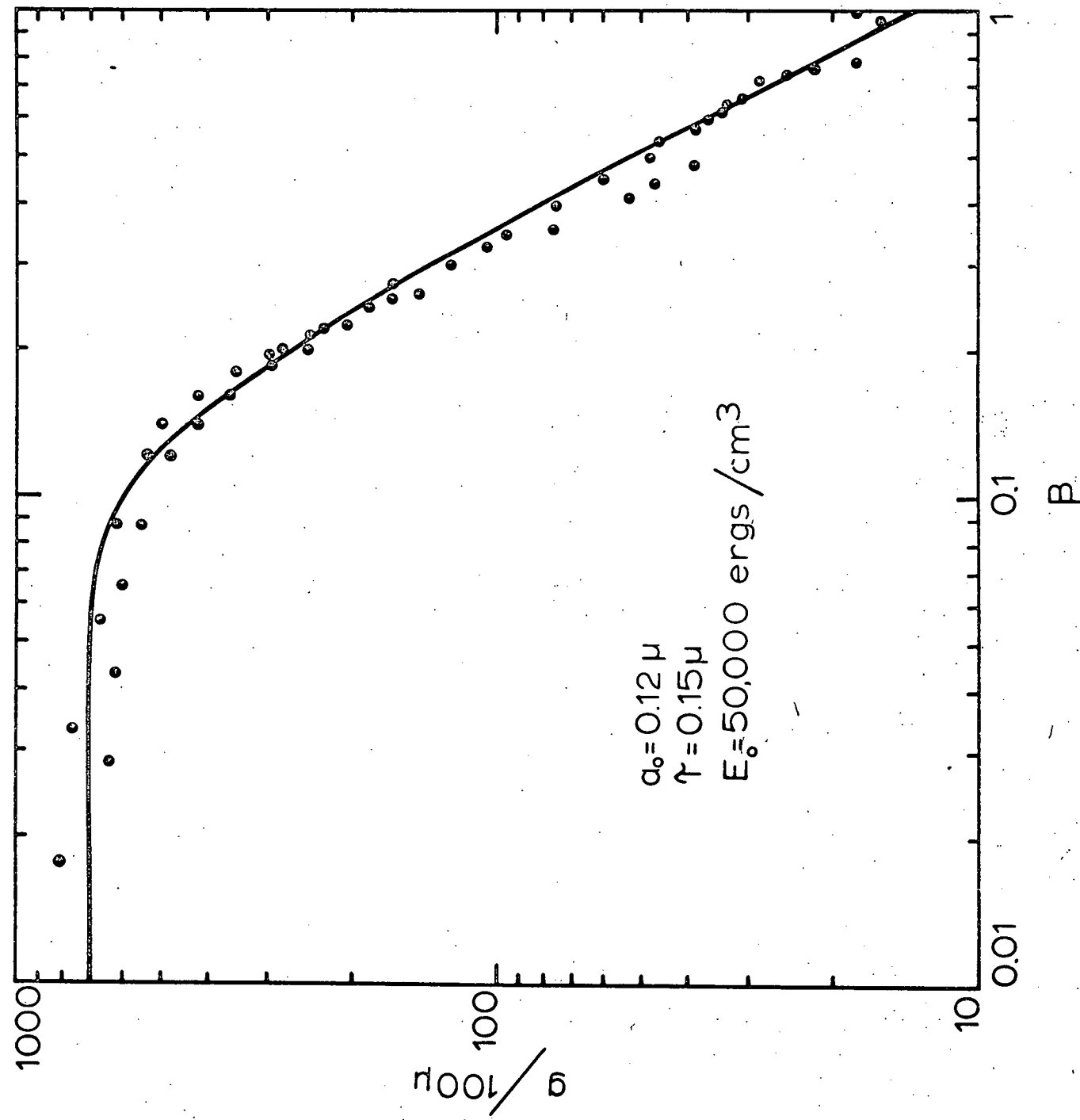
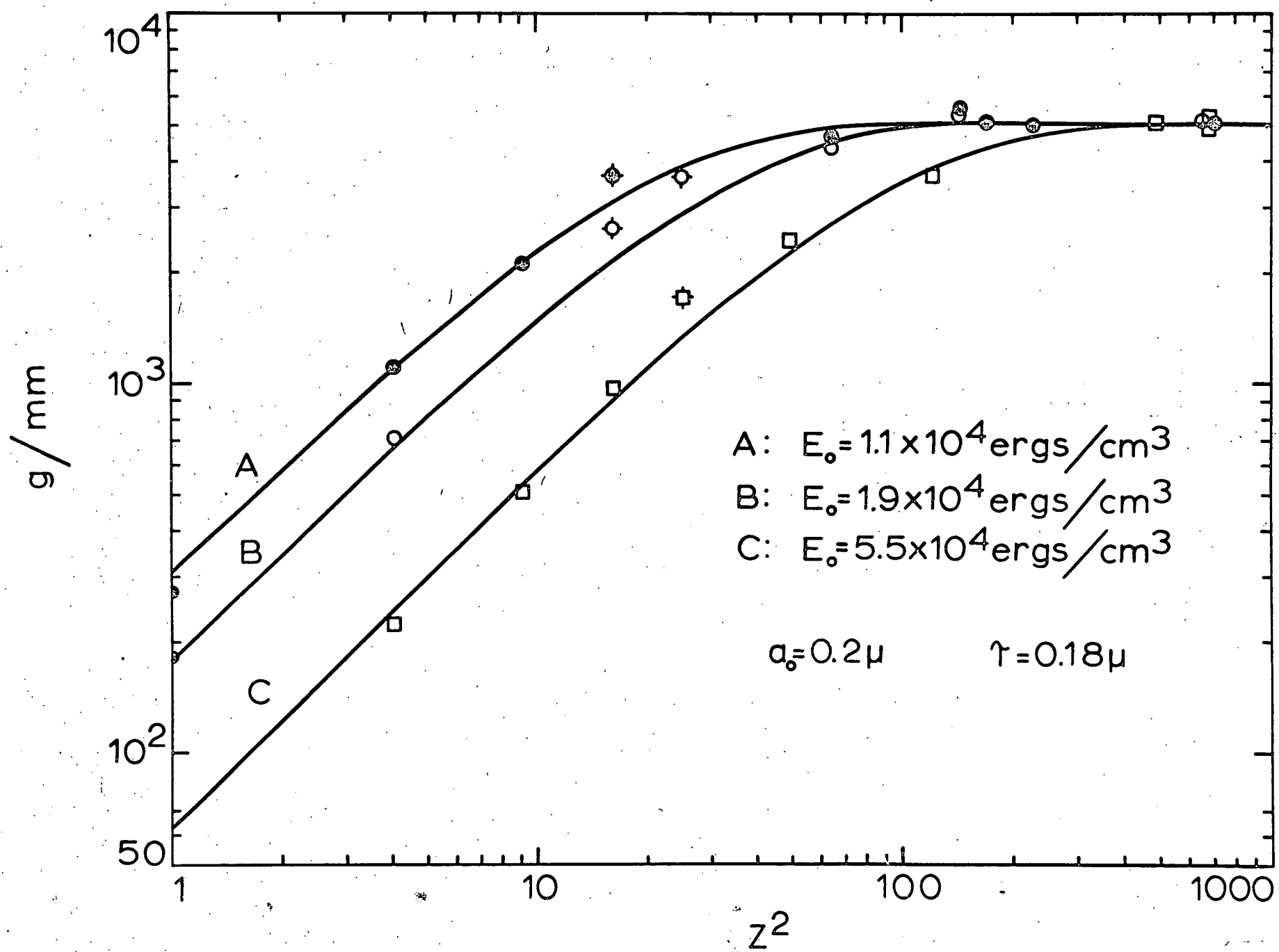


Fig. 6.

Fig. 7

23





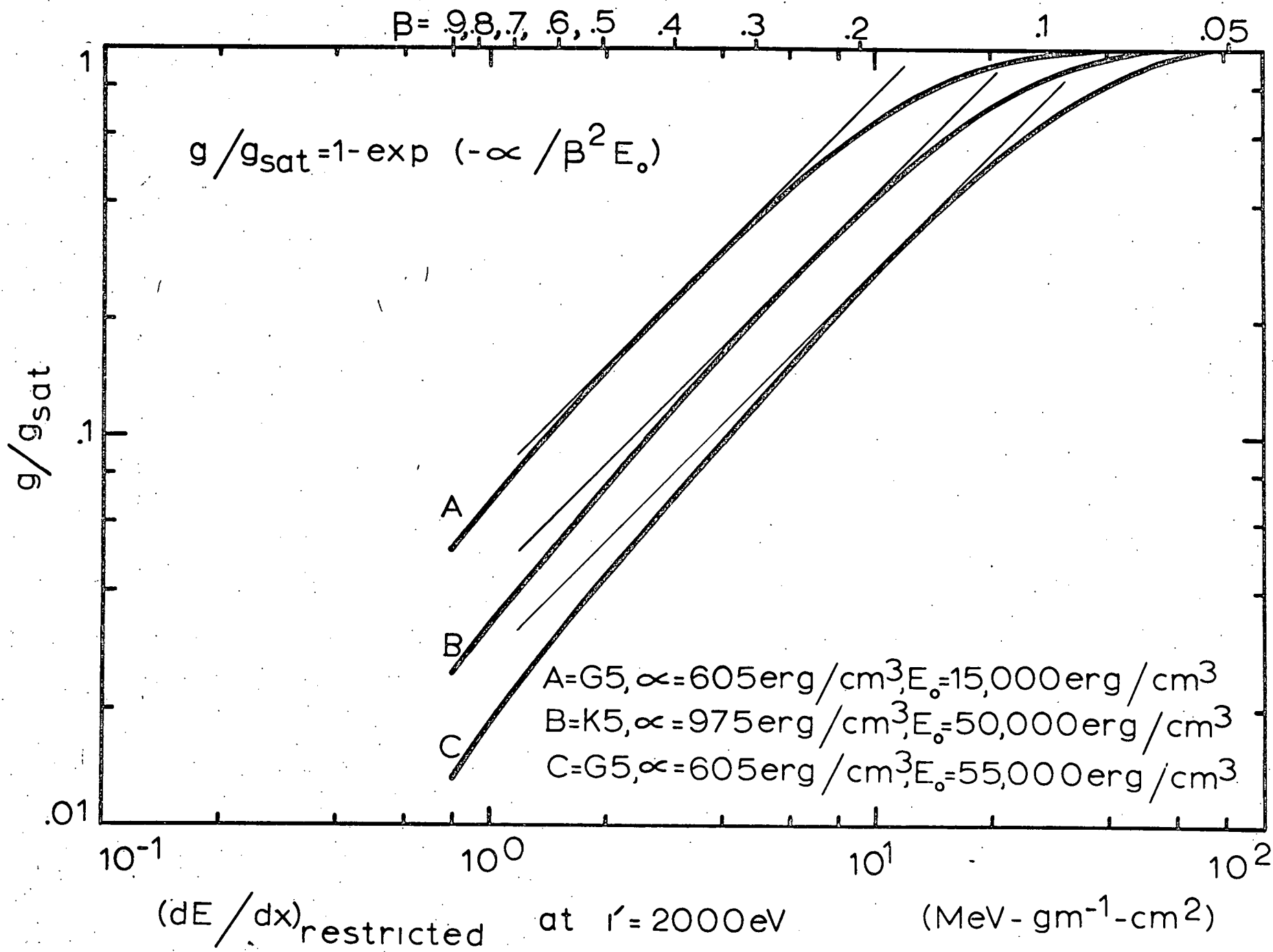


Fig. 9

RELATIVE PULSE HEIGHT

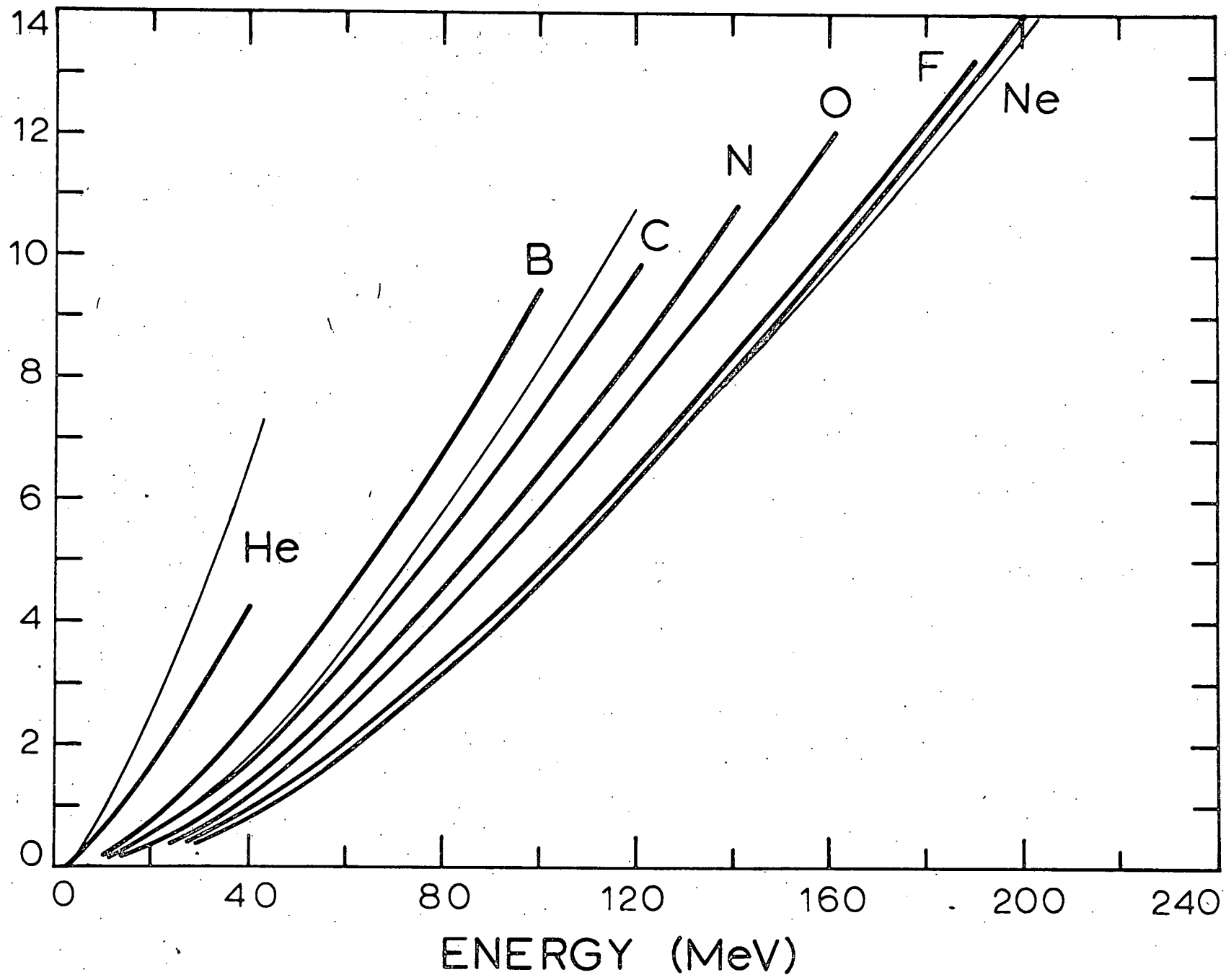
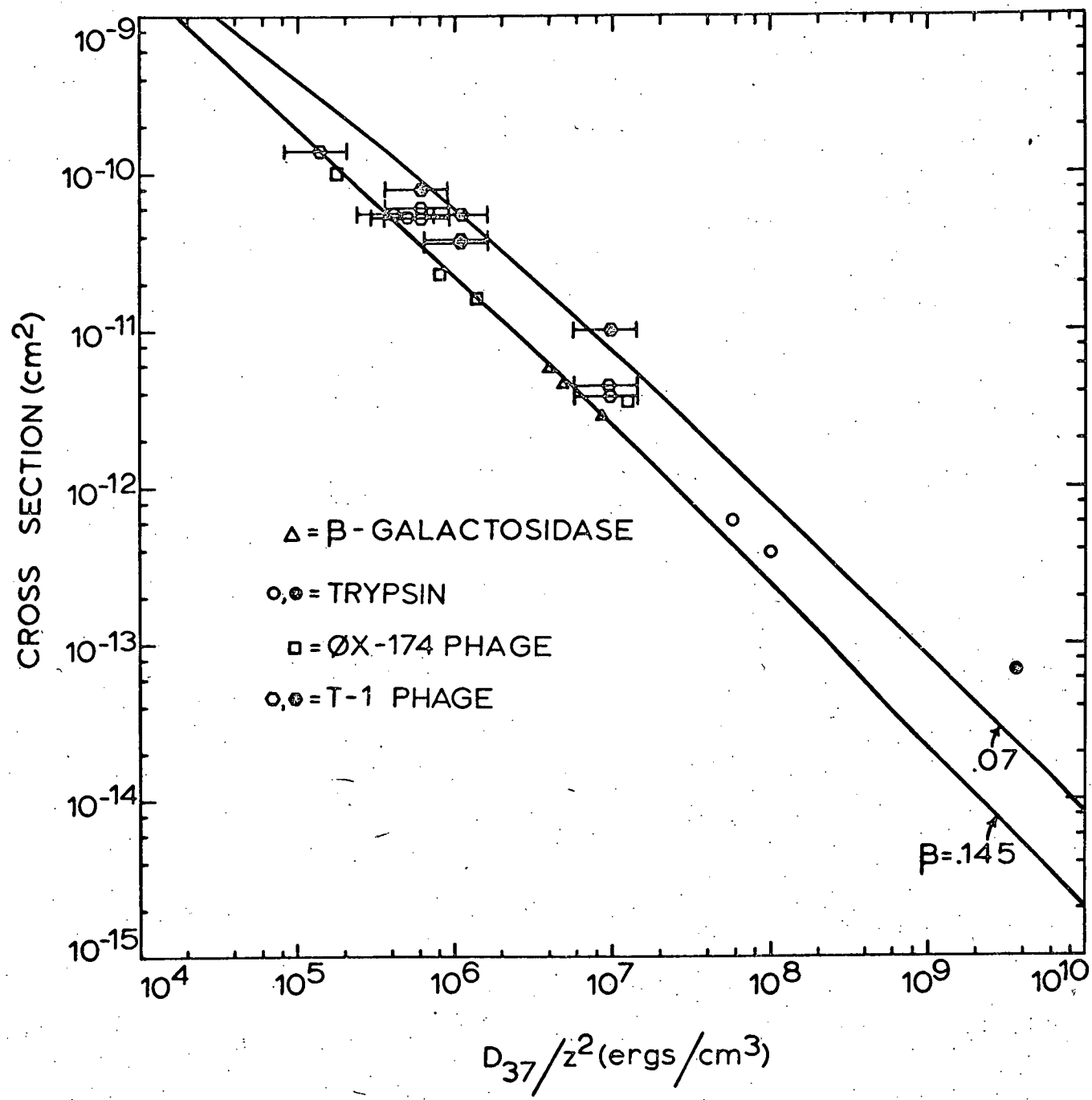


Fig. 10

Fig. 11

27



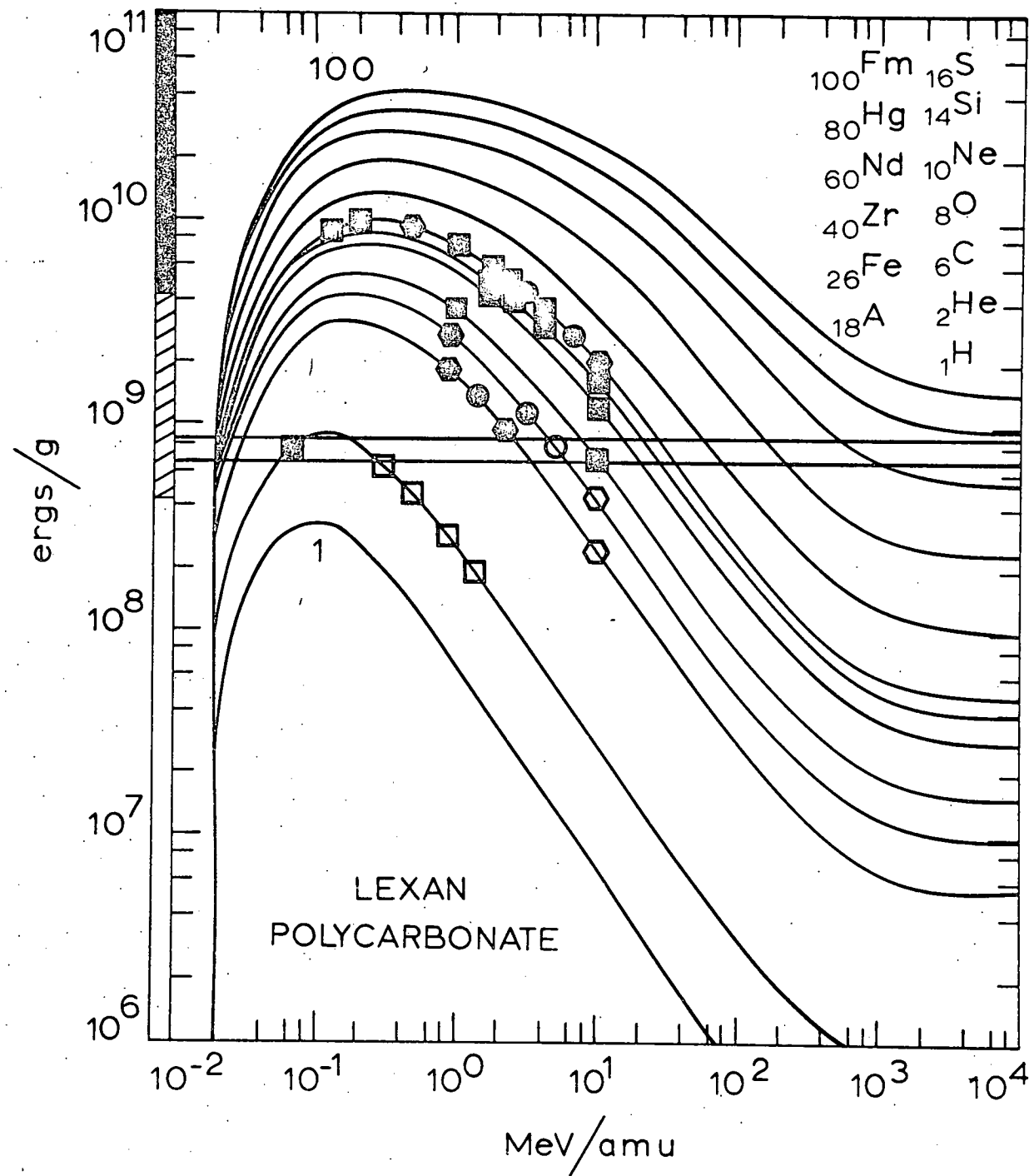


Fig. 12 28